Journal of Inclusion Phenomena and Macrocyclic Chemistry **41:** 53–59, 2001.

Crown-Appended Cholesterol Gelators and Transcription of their Superstructures to Silica Gel

JONG HWA JUNG* and SEIJI SHINKAI**
Chemotransfiguration Project, Japan Science and Technology Corporation (JST), 2432 Aikawa, Kurume, Fukuoka 839-0861, Japan

(Received: 15 July 2001; in final form: 31 August 2001)

Key words: cholesterol, crown, organogel, silica, sol-gel, transcription, TEOS

Abstract

The design of artificial models of the 'biomineralization' processes utilizing sol-gel polymerization has resulted in the union of inorganic materials research and supramolecular organic chemistry. This review article introduces the application of crown-appended cholesterol gelators, which have been utilized as versatile building blocks in organogels and as templates for sol-gel transcription. Attention is focused on the use of self-assembled organic superstructures to the creation of novel inorganic materials with controlled morphologies.

Introduction

The use of organic molecules, assemblies and supramolecular systems in the development of novel inorganic materials continues to offer new and exciting alternatives to conventional synthetic strategies [1]. Since these higher-order aggregates can provide various architectures, sol-gel polymerization utilizing them as templates results in various novel inorganic architectures which cannot be created directly from inorganic materials. As possible templates, protein, multicellular superstructures, surfactants and DNA have been utilized to create such novel structures of inorganic materials [2–4].

Low-molecular-weight organic gelators have been the focus of much attention in recent years [6–10]. The gelator molecules self-assemble through highly specific interaction, allowing preferential one-dimensional growth, usually to form fibers, strands, or tapes. Thus, solids in these gels differ from common crystals, for which the ratio of dimensions of small and large crystals is usually nearly constant. The elongated objects join in three-dimensional networks that encapsulate the liquid component and inhibit its flow. The property of organogelation usually arises from the self-assembly of small molecules utilizing noncovalent interactions such as hydrogen-bonding, π–π stacking, or charge-transfer interactions, into fibers which like polymer gels, become entangled, trapping solvent molecules. The formation of these self-assembling fibers requires a stabilizing intermolecular interaction and represents a balance between the tendency of the molecules to dissolve or to precipitate in a given solvent.

More recently, it was found that certain cholesterol derivatives can gelate even tetraethoxysilane (TEOS), which results in silica gel by sol-gel polymerization [7, 11]. Very interestingly, it was shown that sol-gel polymerization of gelated TEOS solutions followed by calcination affords novel silica with a hollow fiber structure because the organogel fibers act as a template to create an inside tube in the polymerization process [11]. A cationic charge of organogel is necessary to sol-gel transcription into silica gel. However, the introduction of a cationic group into organogelators tends to reduce the gelation ability and these systems scarcely result in the controlled superstructures. An idea to overcome this dilemma came to our mind: that is, the cationic charge can be readily incorporated by a metal-crown interaction. We have found that crown-appended cholesterol gelators not only display various superstructures such as lamellar, linear-fiber, vesicular, and helical-ribbon structures, but also act as good templates in sol-gel polymerization. In this review we survey various superstructures of crown-appended gelators formed by self-assembly and their sol-gel transcription to silica gel.

* Present address: CREST, Japan Science and Technology Corporation (JST), Nanoarchitectonics Research Center, National Institute of Advanced Industrial Science and Technology (AIST), Tsukuba Central 4, 1-1-1 Higashi, Tsukuba, Ibaraki 305-8562, Japan.
** Author for correspondence.

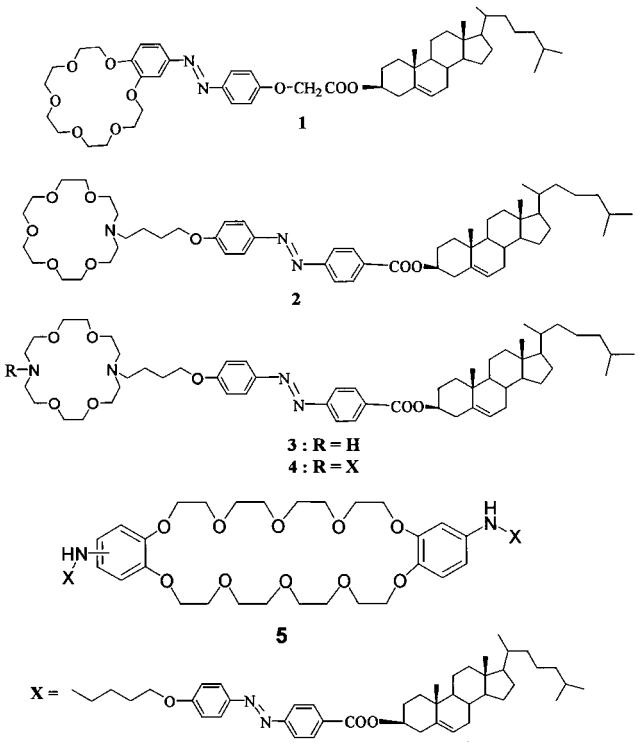

Superstructures of organogelators

The gelators can be classified into two categories according to the driving force for molecular aggregation: hydrogen-bond-based gelators and nonhydrogen-bond-based gelators [6–10]. Typical examples of the former are aliphatic amide- or urea-based cyclohexanediamine and sugar-based derivatives, which showed unique helical structures in their fibrous aggregates formed in certain solvents [10]. Typical examples of the latter are cholesterol derivatives [6]. Aggregation of these compounds is based upon π–π stacking, van der Waals force, and solvophobic effects

In these gel-forming aggregates, the crown ether groups play the following essential roles: that is (i) because of their chain flexibility, introduction of a crown ether group suppresses the formation of crystalline precipitate and rather enhances the gelation ability, (ii) oxygen (and nitrogen) atoms in the (aza)crown ring can act as a silica binding site with the hydrogen-bonding interaction; moreover, when the crown ring binds metal cations or the nitrogen is protonated, they can bind anionic silica particles with the electrostatic interaction, and (iii) they can act as a guest binding site which affects the gelation properties. In this section, we survey the gelation properties of crown-integrated gelators and their roles in the sol-gel transcription processes.

Organogel morphologies

Images of molecular aggregates can be observed on an electron microscope, because the first stage of physical gelation is self-aggregation of gelator molecules. The superstructures constructed in the organogel **1**, which has a benzo-18-crown-6 moiety, were observed by SEM. The xerogel featured a fibrous network structure with 25∼62 nm diameter and the fibers were partially twisted in a helical fashion (arrows in Figure 1a). In contrast, the SEM image of xerogel **2** did not show the fibrous structure characteristic of organogel systems but rather featured film-like aggregates with 30∼40 nm thickness. One may regard that these films consist of the lamellar structure of **2**. It is noteworthy that some films are curved (arrows in Figure 1b) to form a pseudo-cylindrical structure. The most interesting is the xerogel obtained from a **3**+cyclohexane system. As shown in Figure 1c, the xerogel featured a tubular structure with 45∼75 nm wall thickness and 170∼320 nm inside tube diameter. Careful examination of this picture reveals that the wall consists of a multi-layer structure. Presumably, the curved lamellae as seen for **2** have developed to roll up to a tubular structure. It is not clear, however, why the growth of the curved lamellae stops in **2** whereas it continues to grow up to the 'roll-paper-like' structure in **3**.

Gokel and co-workers found that certain azacrown-appended cholesterol derivatives can form unique vesicular or lamellar structures in the absence and the presence of metal salts in aqueous solution [12–14]. They possess a polar azacrown head group and a suitable hydrophobic group to form stable aggregates, and the aggregate morphology can be adjusted by the ring size of the azacrown head group or the length of the hydrophobic group. It thus occurred to us that these superstructures created from the azacrown-appended cholesterol derivatives might be useful as a template for the sol-gel transcription into the silica structure.

We observed the structure of the xerogel sample **4** prepared from acetic acid by SEM and TEM. **4**+acetic acid gel results in two different spherical structures, one with ca. 200 nm diameter and the other with ca. 2500 nm diameter (Figures 1d and 1e). The spherical morphology makes a sharp contrast from more common forms of organogels, fibrous or plate-like. Further interesting is the finding that the smaller vesicles are connected to one another like a pearl necklace. So far, it has been believed that the fibrous aggregates are indispensable to gelation. Presumably, this new class of cross-link in the present system can be also the origin of the gelation phenomena. When **4**+acetic acid gel was dissolved by heating and sonicated by a 35 watts tip sonicator for 15 min, the resultant SEM picture shows the increase in the concentration of the larger vesicle. One particle was cut by ultramicrotome. It is seen from Figure 1e that the particle has a shell wall of ca. 200 nm thickness and an inner sphere of ca. 300 nm. The clearer image of the larger vesicle was obtained from the TEM pictures. The **4**+acetic acid gel was translucent even in the presence of uranyl acetate, which was subjected to the TEM observation. The TEM picture (Figure 1e) clearly established that the shell wall consists of the multi-layered structure with ca. 5 nm layer thickness and 200∼350 nm diameter.

On the other hand, Figure 1f shows a TEM picture of the organogel **5** obtained from acetic acid. Very interestingly, the organogel **5** bearing a 30-crown-10 moiety mainly consists of the tubular structures with ca. 520 nm outer diameter but

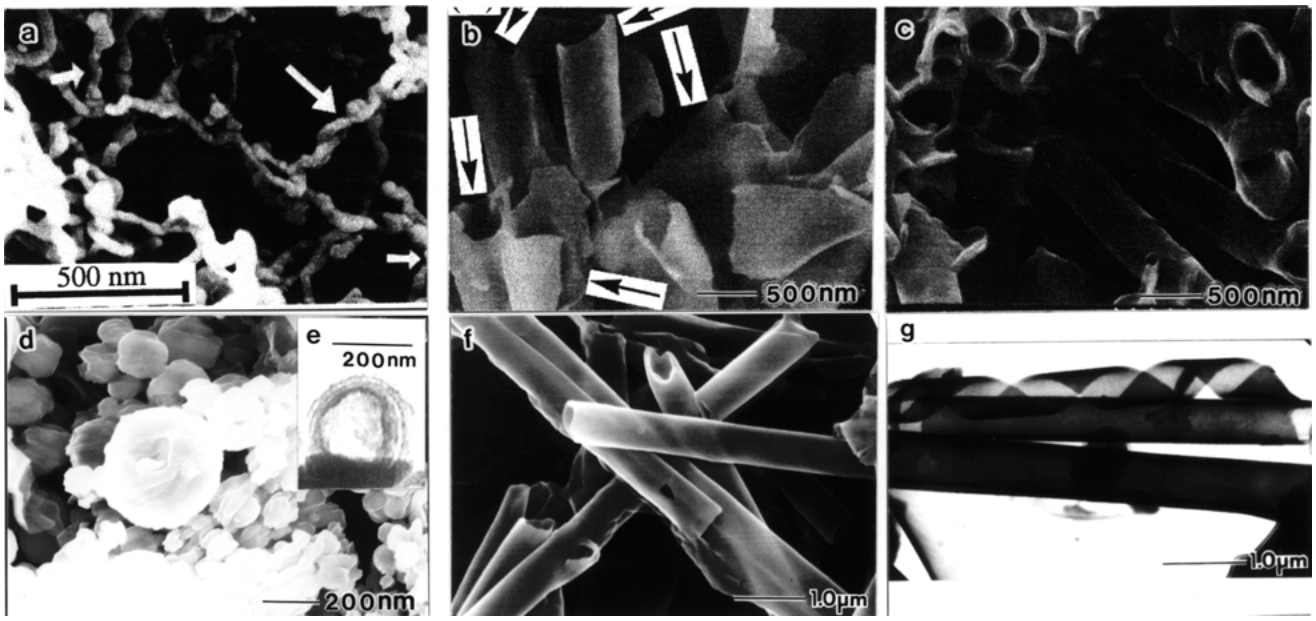

Figure 1. SEM images of xerogels prepared from (a) the cyclohexane gel **1**, (b) cyclohexane gel **2**, (c) cyclohexane gel **3**, (d) acetic acid gel **4**, TEM image of (e) acetic acid gel **5** (negatively stained by UO_2^{2+}), and SEM (f) and TEM (g) images of acetic acid gel **5** (negatively stained by UO_2^{2+}).

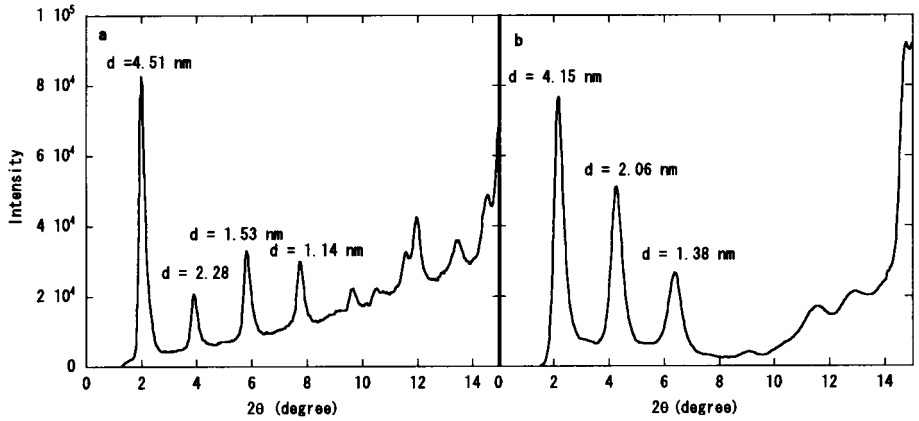

Figure 2. Powder XRD spectra of xerogels (a) **2** and (b) **3**.

Table 1. Conditions for sol-gel polymerization of TEOS and resultant silica structures

Run	Gelator[a]	[$KClO_4$] /mmol	Major solvent	Silica structure[b]
1	**2**	40	1-butanol	tubular
2	**2**	20	1-butanol	tubular
3	**2**	3	1-butanol	granular
4	**2**	0	aniline	granular
5	none	40	1-butanol	granular

[a][Gelator] = 40 mmol.
[b]The tubular structure was observed both by TEM and SEM whereas the granular structure was observed only by SEM.

also illustrates the linear ribbon, and the helical ribbon with 1700–130 nm pitch. In addition, the SEM picture of the xerogel **5** also reveals the characteristic tubular structure (Figure 1g). These results indicate that the structure of this organogel involves several metastable intermediate processes, viz. the linear ribbon → the helical ribbon → the tubule. To the best of our knowledge, this is the first observation for the growing process of these superstructures in the organogel system.

X-ray diffraction

Recently, an X-ray crystallographic methodology for ascertaining the molecular packing of gelators in the gel phase has been reported, and this method is being used to clarify the gelation mechanism of low-molecular-weight gelators [16–17]. However, the correlation between the molecular packing of gelator molecules and the physical gelation properties is still less understood.

We obtained information about the molecular packing mode of gelator molecules in a neat gel from an X-ray diffraction pattern of the xerogel. The diffraction patterns are characterized by four and three sharp reflection peaks of 4.51 nm, 2.21 nm, 1.52 nm and 1.1 4 nm for xerogel **2** (Figure 2a), and 4.11 nm, 2. 06 nm and 1.81 nm for xerogel **5** (Figure 2b), respectively, the relative intensity of which is almost exactly in the ratio of 1/2 : 1/3 : 1/4. These mean that xerogels **2**

and **5** maintain a multi-layered structures with the interlayer distance of 4.51 nm and 4.40 nm corresponding to the (100) plane, respectively. However, the X-ray pattern of solids **2** and **5** did not give any sharp peaks. These results support the view that the organogel structures are well-ordered multi-layered structures in the present systems.

Sol-gel transcription

The tubular structure of the silica

Very recently, we have successfully transcribed organogel superstructures into the silica gel by sol-gel polymerization [12]. It was found that the cationic charge of organogels is indispensable to sol-gel polymerization. The sol-gel polymerization was carried out as follows. Compound **1** (5.1 $\times$ 10^{-6} M) and $KClO_4$ (for the amount see Table 1) were dissolved in dichloromethane (3.0 g). The solution was evaporated to dryness. Run 1 containing the high concentration of $KClO_4$ results in the fibrous silica as shown in a SEM picture of Figure 3a. To see the inside of this fibrous silica the TEM picture was taken (Figure 3b). Similar SEM and TEM pictures were also obtained from Run 2, but the silica structure obtained from Run 1 (outer diameter ~50 nm, inner diameter ~3 nm) was smaller than that obtained from Run 2 (outer diameter 30~200 nm, inner diameter ~50 nm). In Run 3 where sol-gel polymerization was carried out at the low $KClO_4$ concentration, in contrast, the resultant silica only showed the conventional granular structure similar to that prepared from a solution in the absence of the gelator (Run 5). The 1-butanol solution was not gelated by **1** in the absence of $KClO_4$. Since **1** could gelate aniline, we performed the same sol-gel polymerization in aniline/TEOS/water/benzylamine = 45.0/15.0/5.7/5.6 (mg; Run 4). Again, the product was the granular silica. The foregoing results consistently support the view that the construction of the hollow fiber silica is profoundly related to the specific K^+-benzo-18-crown-6 interaction.

On the other hand, interestingly, sol-gel polymerization in 1-butanol gels of **2** and **3** resulted in a tubular structure even in the absence of metal salt (Figure 4). Judging from the foregoing information obtained from an insight into the origin of the hollow fiber silica formation, we consider that this structure is also due to the cationic charge arising from protonation of the monoaza- and the diaza-18-crown-6. Since their pK_a values are relatively high [18], they should be partially protonated under the sol-gel polymerization conditions. To neutralize this cationic charge, we added a small amount of Et_4NOH (tetraethylammonium hydroxide: 3 equivalents to **2** or **3**). As expected, the silica obtained from **3** was changed to the conventional granular structure. The result again supports the importance of the cationic charge in the creation of hollow fiber silica. In contrast, **3** still yielded the hollow fiber silica even in the presence of Et_4NOH. Since the pK_a for diaza-18-crown-6 (3.64) is higher than that for monoaza-18-crown-6 (ca. 2.0~3.20) [18], a trace amount of the cationic charge still

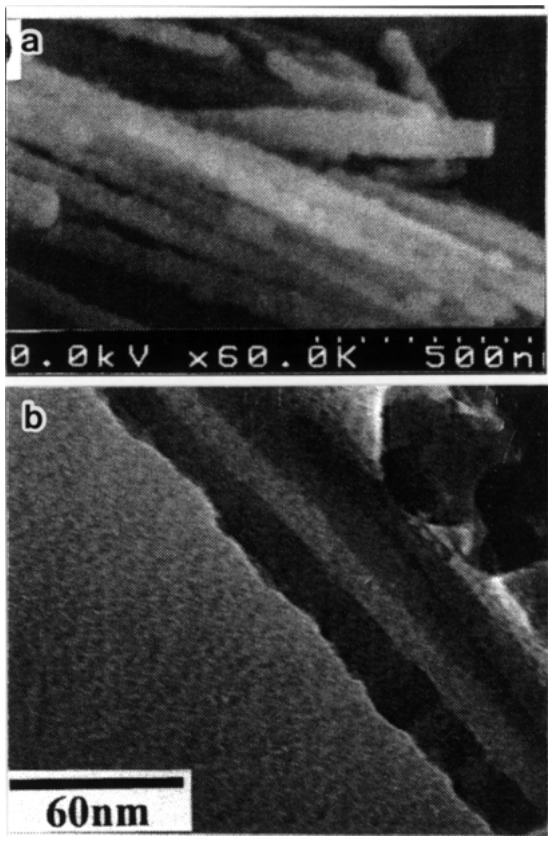

Figure 3. (a) SEM and (b) TEM images of the silica obtained from **1** in the presence of $KClO_4$.

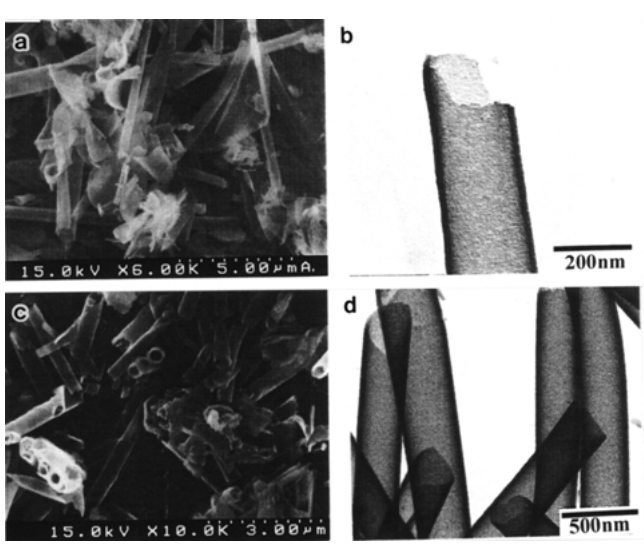

Figure 4. SEM and TEM images of the silica obtained from **2** (a and b) and **3** (c and d) in the absence of metal.

remains in the gel fibers of **3**, which eventually plays a role to create the hollow fiber silica.

TEM pictures of the silica were observed after removal of **2** and **3** by calcination. The surface of the hollow fiber silica obtained from **2** and **3** is smooth and the tube wall is rather thin, giving rise to a large inner diameter (Figures 4b and 4d). Presumably, sol-gel polymerization of TEOS proceeds along the surface of the lamellar aggregates of the organogels (Figures 1b and 1c) to grow up as a tubular structure.

This view is further supported by sol-gel polymerization in the presence of metal salts. As shown in the SEM and TEM pictures in Figures 3a and 3b, the tube wall of the silica obtained from **2** features a roll-paper-like multi-layer structure. The tube wall of the silica obtained from **3** (Figures 4c and 4d) is thinner than that from **2**. However, careful observation of the tube end reveals that these silica fibers also have the multi-layer structure.

Vesicular structure of the silica

Mesoporous inorganic materials with vesicular structures have received special attention because of their potential applications as sorption media, molecular sieves, and catalysts [19–22]. However, all vesicular (multi-layered) mesostructures reported to date had shells of undesirable thickness and shape. The earliest approach to the vesicular structure of inorganic materials was reported by Ozin *et al.* who synthesized a lamellar aluminophosphate phase in a solution containing vesicles formed from tetraethylene glycol, amphiphilic alkylamines and water [21–22]. The resulting material was composed of millimeter-sized spheroids with patterned surfaces. In addition, recently, Pinnavaia and coworkers reported that arrangements of mesoporous inorganic materials with vesicular structures which showed 3∼70 nm of thin shells have been accomplished by 'gemini'-type surfactants as templates in aqueous solution [19–20]. However, these particles have shells that consist of uni- and multilamellae. Therefore, we carried out sol-gel polymerization to obtain a unique vesicular structure of the silica using organogel **4** as a template [23].

Figure 5a shows the SEM micrographs of the silica taken after calcination. From **4**+acetic acid gel, the spherical silica structures are yielded. As expected, one can observe both the cross-linked smaller particles with ca. 200 nm diameter and the isolated larger particles with ca. 2500 nm in diameter. Figure 5a accidentally catches one broken particle (the smaller particle is shown in the left image and the larger particle is shown in the right image). It is seen from these images that the inside of these particles have a cavity inside. Presumably, this breakage is induced by the vacuum necessary to the SEM sample preparation. After sectioning with an ultramicrotome, the edge of the small particle was observed with TEM (Figure 5c). It is seen from this TEM image that the shell wall consists of multi-layered lamella having a 5 nm spacing. These results clearly support the view that the multi-layered structure of the organogels is precisely transcribed into the silica structure.

Helical ribbon structures of the silica

Kunitake and coworkers found that certain amphiphiles can form the tubular structure through the helical ribbon structure in aqueous solution [24]. They possess a polar head and a suitable chiral hydrophobic group to form stable aggregates. It thus occurred to us that judging from the versatility of crown-appended cholesterol-based gelators [6, 25, 26], one might be able to find both structures, growing from the helical ribbon to the tubule (as suggested by Kunitake *et al.*

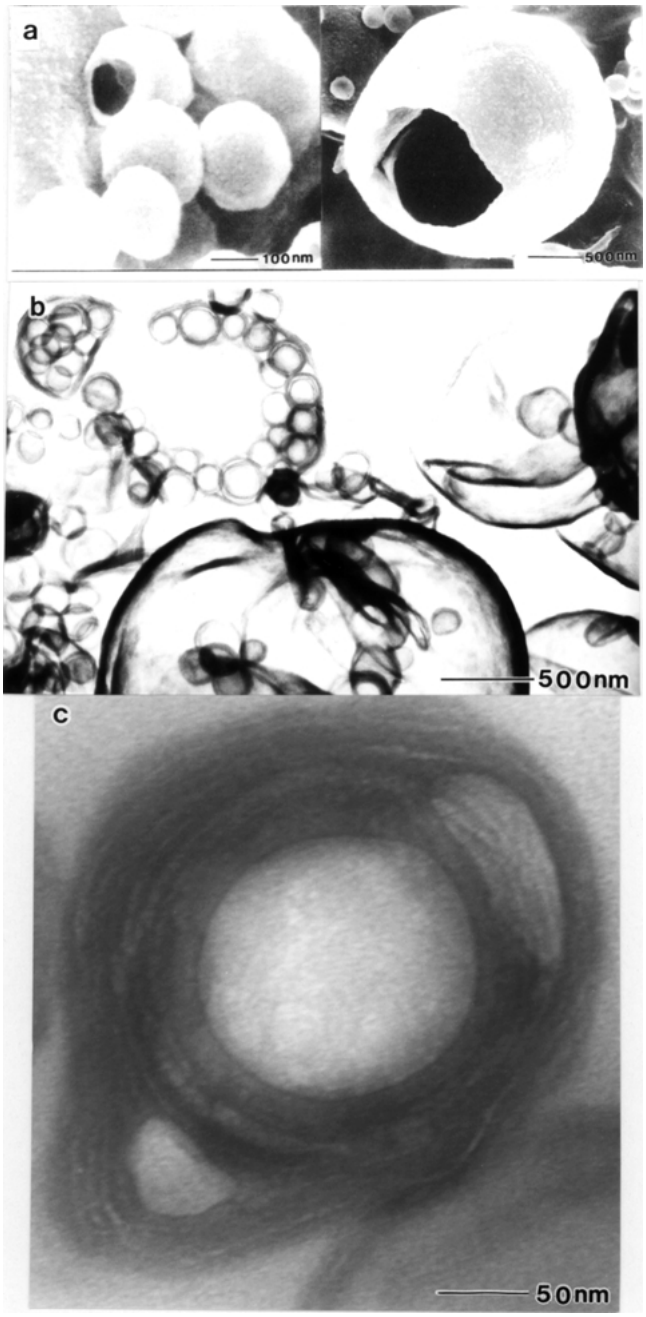

Figure 5. SEM (a and b) and TEM (c) images of the silica obtained from **4**.

[24] for the aqueous solution system). With these objects in mind, we have designed compound **5**, which has two cholesterol skeletons as a chiral aggregate-forming site, two amino groups as an acidic proton binding site, and one crown moiety as a cation binding site [27].

Figure 6a shows a SEM picture after calcination: the silica obtained from **5**+acetic acid possesses the helical ribbon structure with 1700–1300 nm pitches and the tubular structure of the silica with ca. 560 nm outer diameter. As far as can be recognized, all the helicity possesses a right-handed helical motif. Since the exciton-coupling band of the organogel also showed R (right) helicity by CD, we consider that a microscopic helicity is reflected by a macroscopic helicity. These results indicate that the novel helical

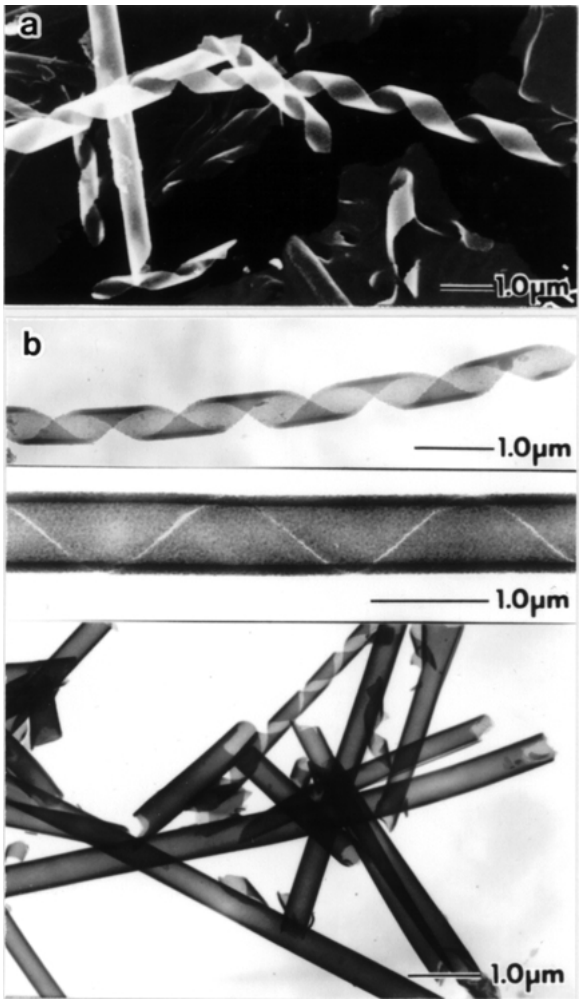

Figure 6. SEM (a) and TEM (b) images of the silica obtained from **5** after calcination.

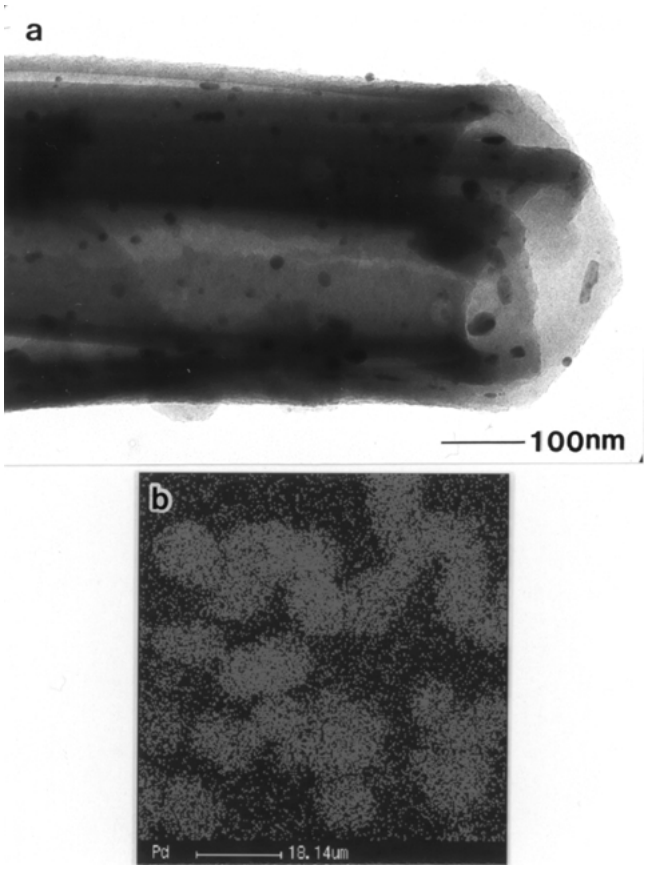

Figure 7. TEM (a) image of the silica obtained from **2** in the presence of $AgNO_3$ and EPMA image (b) of the silica obtained from **4** in the presence of $Pd(NO_3)_2$: palladium map.

ribbon structure and the tubular structure of the organogel have successfully been transcribed into the silica structures. TEM pictures were taken after removal of **5** by calcination (Figure 6b). Very interestingly, 1700–1300 nm of the helical pitches of the helical ribbon structure remained constant with a gradual change into the tubular structure. In addition, the silica illustrated double layers with an interlayer distance of 8–9 nm. These results indicate that TEOS (or oligomeric silica particles) was adsorbed onto both surfaces of the double-layered tubules with 8–9 nm thickness. Therefore, the tubular silica possesses two hollow cavities. The smaller hollow with 5 nm layers was created by organogel template whereas the larger hollow with 460–430 nm inner diameters was created by the growth of helical ribbon. We believe that such a precise transcription becomes possible for the first time by using the organogel superstructures as a template featuring the crystal-like characters.

Deposition of noble metals

It is known that azacrown moiety has a high affinity for soft metals [19]. Particularly, **2** and **4** bearing the monoazacrown moiety and the diaza-crown moiety should act as good ligands. When sol-gel polymerization of TEOS is carried out in the presence of these metal-binding species, metals could be deposited on the surface of the resulting silica after calcination. With this intriguing idea in mind, sol-gel polymerization of **2** and **4** was carried out in the presence of $AgNO_3$ and $Pd(NO_3)_2$. The TEM picture of the silica obtained from **2** in the presence of $AgNO_3$ thus obtained is shown in Figure 7a [28]. In case of the silica prepared from **2** in the presence of $AgNO_3$, careful examination of Figure 7a reveals that there are many small dots (0.5∼1 nm) on the silica wall. In some cases they aggregate into large particles (20∼55 nm), which are clearly seen to be mostly deposited between the silica layers. X-ray electron probe microanalyzer (EPMA) clearly shows that Pd is deposited on the silica surface, the content being 1.8 wt7b) [25]. The results indicate that the azacrown-appended gelators are useful as a new metal-deposition method on the silica matrix.

Conclusions

Chemistry working at the interface of organic and inorganic chemistry has developed several techniques recent years that have enabled the synthesis of inorganic materials with controlled morphologies. In this review, we have presented the use of four different organic assemblies: fibers, lamellae, vesicles, and helical ribbon for crown-appended cholesterol gels, which have successfully been transcribed into silica

materials. The potential prospects for the future include the design of more elaborate templates with the ability both to dictate the shape of the inorganic materials and to organize the particles into the desired fashion. In this work not only will a greater understanding of the biological materials be reached but novel materials with useful properties will also be created.

References

1. S. Mann: *Biomimetic Materials Chemistry*, S. Mann (ed.), VCH, New York (1996).
2. W. Shenton, T. Douglas, M. Young, G. Stubbs, and S. Mann: *Adv. Mater.* **11**, 253 (1999).
3. T. Douglas and M. Young: *Nature* 393, 152 (1998). W. Shenton, D. Pum, U. Sleytr, and S. Mann: *Nature* **389**, 585 (1997).
4. S.A. Davis, S.L. Burkett, N.H. Mendelson, and S. Mann: *Nature* **385**, 420 (1997).
5. M. de. Loos, J. van. Esch, I. Stokroos, R.M. Kellogg, and B.L. Feringa: *J. Am. Chem. Soc*. **119**, 12675 (1997).
6. K. Murata, M. Aoki, T. Suzuki, T. Harada, H. Kawabata, T. Komori, F. Ohseto, K. Ueda, and S. Shinkai: *J. Am. Chem. Soc.* **116**, 6664 (1996); S. Shinkai and K. Murata: *J. Mater. Chem.* 485 (1998); K. Inoue, Y. Ono, Y. Kanekiyo, T. Ishi-I, K. Yoshihara, and S. Shinkai: *J. Org. Chem.* **64**, 2933 (1999).
7. P. Terech, I. Furman, and R.G. Weiss: *J. Phys. Chem.* **99**, 9558 (1995) and references cited therein.
8. K. Yoza, N. Amanokura, Y. Ono, T. Akao, H. Shinmori, M. Takeuchi, S. Shinkai, and D.N. Reinhoudt: *Chem. Eur, J.* **5**, 2722 (1999); K. Yoza, Y. Ono, K. Yoshihara, T. Akao, H. Shinmori, M. Takeuchi, S. Shinkai, and D.N. Reinhoudt: *Chem. Commun.* 907 (1998).
9. P. Terech and R.G. Weiss: *Chem. Rev.* **8**, 485 (1997); D.J. Abdallah and R.G. Weiss: *Adv. Mater.* **12**, 1237 (2000).
10. S.W. Jeong, K. Murata, and S. Shinkai: *Supramol. Sci.* **3**, 83 (1996).
11. Y. Ono, K. Nakashima, M. Sano, Y. Kanekiyo, K. Inoue, J. Hojo, and S. Shinkai: *Chem. Commun.* 1477 (1998); Y. Ono, K. Kanekiyo, K. Inoue, J. Hojo, and S. Shinkai: *Chem. Lett.* 23 (1999).
12. L.E. Echegoyen, J. Hernandez, A.E. Kaifer, and G.W. Gekel: *J. Chem. Soc. Chem. Commun.* 836 (1988).
13. A. Nakano, J.C. Hernadez, S.L. Dewall, D.R. Berger, and G.W. Gokel: *Supramol. Sci.* **8**, 21 (1997).
14. L.E. Echegoyen, L. Portugal, S.R. Miller, L. Echegoyen, and G.W. Gokel: *Tetrahedron Lett.* **29**, 4065 (1998).
15. K. Hanabusa, M. Matsumoto, M. Kimura, A. Kakehi, and H. Shirai: *J. Colloid Interface Sci.* **224**, 231 (2000).
16. D.J. Abdallah, S.A. Sirchio, and R.G. Weis: *Langmuir* **16**, 7558 (2000).
17. K. Sakurai, Y. Ono, J.H. Jung, S. Okamoto, S. Sakurai, and S. Shinkai: *J. Chem. Soc. Perkin Trans. 2* 108 (2001).
18. H. Sakamoto, K. Kimura, and T. Shono: *J. Org. Chem.* **51**, 5974 (1986).
19. P.T. Tanev, Y. Ling, and T.J. Pinnavaia: *J. Am. Chem. Soc.* **119**, 8616 (1997).
20. S.S. Kim, W. Zhang, and T.J. Pinnavaia: *Science* **282**, 1302 (1998).
21. G.A. Ozin: *Acc. Chem. Res.* **30**, 313 (1997).
22. S. Oliver, A. Kuperman, N. Coombs, and G.A. Ozin: *Nature* **378**, 47 (1995).
23. J.H. Jung, Y. Ono, K. Sakurai, M. Masahito, and S. Shinkai: *J. Am. Chem. Soc.* **122**, 8648 (2000).
24. N. Nakashima, S. Asakuma, and T. Kunikata: *J. Am. Chem. Soc.* **107**, 509 (1985).
25. J.H. Jung, Y. Ono, and S. Shinkai: *Langmuir* **16**, 1643 (2000).
26. J.H. Jung, H. Kobayashi, M. Masuda, T. Shimizu, and S. Shinkai: *J. Am. Chem. Soc.* In press.
27. J.H. Jung, Y. Ono, and S. Shinkai: *J. Chem. Soc., Perkin Trans. 2* 1289 (1999).